Supporting material

Exploring the Relative Bending Status of a CVD Graphene Monolayer with Gap-Plasmon

Young Hwan Min and Won-Hwa Park*

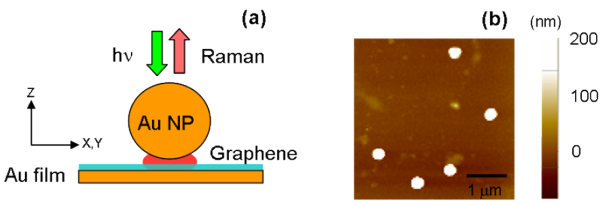

Figure S1. (a) Experimental setup and sample structure. The illumination and detection are carried out in the epi-direction using up-right microscope system. (b) Atomic Force Microscope (AFM) image of Au NP-graphene-Au film system

Figure S1(a) shows the experimental configuration. A gold thin-film with thickness of 10 nm is formed on a cleaned glass substrate by thermal evaporation. The separate Atomic Force Microscope (AFM) measurement found the typical rms roughness of the film to be less than 0.2 nm. We employ a dry-transfer process for the graphene film using a soft substrate such as polymethyl methacrylate (PMMA) stamp.[33] Here we first attach the PMMA stamp to the CVD-grown graphene film on the Cu substrate. The Cu substrate can be etched away using $FeCl_3$, leaving the adhered graphene film on the PMMA substrate. After cleaning with DI water, we can transfer a FLG film to the Au substrate. After transferring graphene onto the Au film, a drop of Au colloidal nanoparticle solution (nominal diameter ~200 nm, BB International) is applied (~15 μL) onto the graphene-Au film, followed by rinsing and air-drying at ambient temperature. Figure S1(b) shows the AFM image of Au NP-graphene-Au film system.

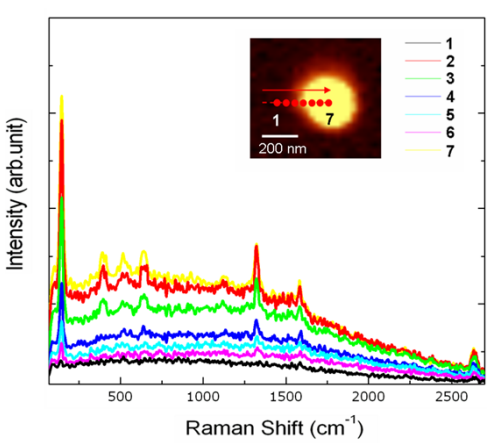

Figure S2. (a) SERS spectra obtained from #1 to #7 domains shown in the inset image. Bright circle type shows the SERS image gated at LBM peak.(inset) Note that the only LBM peak is started to emerge abruptly at low-wavenumber region. (< 700 cm^{-1})

Figure S2 shows the SERS spectra of FLG along with the numbered axis from inset image. The number of graphene layer may be deduced nearly 5 layers considering the LBM peak position.[35] From #1 to #7, the Raman intensities of each phonon mode are enhanced with the accompanied background as approaching to the center of the junction. The #1 point, where uttermost region from Au NP, exhibits narrowly weak 2D and G mode Raman signal. By approaching the target point to closer to the center of Au NP, Raman signal enhancement of 2D, G and D modes is clearly observed due to electromagnetic (EM) enhancement effect. Specifically, the Raman mode, observed at ~150 cm^{-1} with Full Width at Half Maximum (FWHM) of ~16 cm^{-1} is newly observed with very high signal-to-noise ratio, which is not observed at conventional Raman spectrum at bare Au film or SiO_2/Si substrate as well. Previously, the graphene Raman peak at low-wavenumber (< 700 cm^{-1}) was studied at a few groups. Chun Hung Lui et al reported a comprehensive determination of the different LBM frequencies for FLG by means of the two-phonon overtone spectra observed in doubly resonant Raman spectroscopy from two to 20 layers over the spectral range of 80 ~ 300 cm^{-1}.[34] In particular, the Raman peak at ~ 150 cm^{-1} at Figure 4 from ref 35 maybe coincided with our Raman peak at ~ 150 cm^{-1}. Previously, we could assign that the low-wavenumber SERS peaks were associated with the out-of-plane layer breathing mode (LBM) at the near zone center region and we could interpret that the strongly observed SERS signal at ~ 150 cm^{-1} is ascribed to the LBM of the a FLG.[26,34]

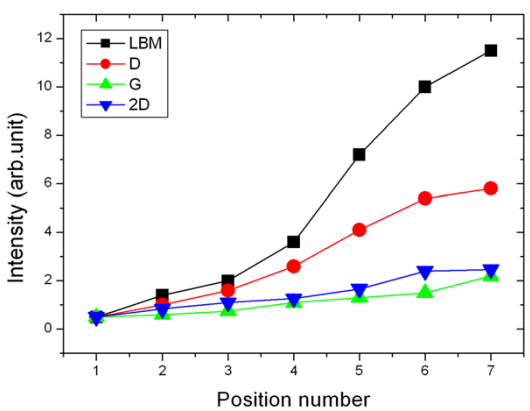

Figure S3. Lateral approach profiles of each phonon mode of FLG from #1 to #7. Dramatic enhancement of SERS intensity from LBM is observed rather than G and 2D modes.

Figure S3 shows the SERS intensity approach profiles of each phonon modes of the FLG from #1 to #7 direction. Interestingly, it is clearly distinguished that approach profiles are phonon mode-dependent. First of all, the enhancement of the SERS intensities of 2D and G modes along with the #1 to #7 is not significantly enhanced, while the LBM mode shows the relatively large increase of SERS intensities along with the #1 to #7 direction than the 2D and G modes. The G mode is associated with the doubly degenerate (iTO and LO) phonon mode (E_{2g} symmetry) at the Brillouin zone center and the vibration is *in-plane* direction. On the other hand, LBM is one of the representative *out-of-plane* phonon modes. It gives us

that the observed LBM mode is considerably and sensitively influenced by the local z-field formed at the near-center of the Au NP-Au film junction in terms of coinciding between z-polarized incident and the LBM phonon axis, leading to dramatic Raman enhancement. However, the G and 2D modes whose vibration is in-plane do not significantly be affected by the incident z-field relatively. Note that D mode shows the moderate SERS enhancement feature. It is well-known that SP^3-type defects are generally displayed as D mode.[10] Not only for in-plane but also out-of-plane defect such as functional group bonding maybe partially influential, resulting in the moderate SERS enhancement of D mode along the z-axis.[34] The SERS enhancement factor per area (nm^2) at Au NP-Au film can be calculated by dividing I(#7) to I(#1) considering the corresponded each focused spot area. The focused area at I(#7) is defined as $\sim\lambda_{exe}/2NA$ while that of the I(#1) can be obtained approximately by the electro-dynamic simulation via Finite Different Time Domain (FDTD) method.[35] Table S1 shows the summarized mode-dependent SERS enhancement factor (EF) per area.

Table S1. Mode-dependent SERS enhancement factor per area (nm^2)

	LBM	G	2D
EF ($/nm^2$)	$\sim 3.0\times10^3$	$\sim 5.5\times10^2$	$\sim 6.4\times10^2$

To conclude, we present that Raman enhancement of a FLG of each phonon mode sandwiched at Au NPs-Au film junctions is different and can be ascribed to the different incident polarization. Closer to the center of the junction, LBM shows dramatic Raman enhancement than the 2D and G modes in terms of coinciding between the z-polarized incident field formed at Au NP-Au film junction and the LBM phonon axis, which can also be quantified that the SERS enhancement factor of the LBM is more than ~ 5.5 times larger than that of the G and 2D modes.

References

1 A. K. Geim, K. S. Novoselov, *Nat. Materials*. **2007**, 6, 183.
2 K. S. Novoselov, A. K. Geim, S. V. Morozov, D. Jiang, Y. Zhang, S. V. Dubonos, I. V. Grigorieva, A. A. Firsov, *Science*. **2006**, 306, 666
3 A. A. Balandin, S. Ghosh, W. Bao, I. Calizo, D. Teweldebrhan, F. Mian, C. N. Lau, *Nano Lett*. **2008**, 8, 902
4 X. Li, W. Cai, J. An, S. Kim, J. Nah, D. Yang, R. Piner, A. Velamakanni, I. Jung, E. Tutuc, S. K. Banerjee, L. Colombo, R. S. Ruoff, *Science*. **2009**, 324, 1312
5 S. Bae, H. Kim, Y. Lee, X. Xu, J.-S. Park, Y. Zheng, J. Balakrishnan, T. Lei, H. R. Kim, Y. I. Song, Y.-J. Kim, K. S. Kim, B. Ozyilmaz, J.-H. Ahn, B. H. Hong, S. Iijima, *Nat. Nanotechnol*. **2010**, 5, 574
6 J. A. Robinson, C. P. Puls, N. E. Staley, J. P. Stitt, M. A. Fanton, K. V. Emtsev, T. Seyller, Y. Liu, *Nano. Lett*. **2009**, 9, 964
7 W.-H. Park, M. Jung, W. Park, J.-S. Moon,S. Noh, T. H. Kim, M. Joo, K. Park, *Appl. Phys. Lett*. **2013**, 103, 033107
8 S. Banerjee, M. Sardar, N. Gayathri, A. K. Tyagi, R. Baldev, *Appl. Phys. Lett*. **2006**, 88, 062111
9 M. Ahmad, S. A. Han, D. H. Tien, J. Jung, Y. Seo, *J. Appl. Phys*. **2011**, 110, 054307
10 A. Eckmann, A. Felten, A. Mishchenko, L. Britnell, R. Krupke, K. S. Novoselov, and C. Casiraghi. *Nano. Lett*. **2012**, 12, 3925
11 Nicklow, R.; Wakabayashi, N.; Smith, H. G. *Phys. Rev. B*. **1972**, 5, 4951
12 M. Mohr, J. Maultzsch, E. Dobardžić, S. Reich, I. Milošević, M. Damnjanović,A. Bosak, M. Krisch, and C. Thomsen, C. *Phys. Rev. B*. **2007**, 76, 035439
13 C. Spudat, M. Müller, L. Houben, J. Maultzsch, K. Goss, C. Thomsen, C. M. Schneider and C. Meyer, *Nano Lett*. **2010**, 10, 4470
14 D. Levshov, T. X. Than, R. Arenal, V. N. Popov, R. Parret, M. Paillet, V. Jourdain, A. A. Zahab, T. Michel, Y. I. Yuzyuk, and J-L Sauvajo, *Nano Lett*. **2011**, 11, 4800
15 S. Kitipornchai, X. Q. He, and K. M. Liew, *Phys. Rev. B*. **2005**, 72, 075443
16 K. Saha, U. V. Waghmare, H. R. Krishnamurthy, and A. K. Sood, *Phys. Rev. B*. **2007**, 78, 165421
17 J.-W. Jiang, H. Tang, B.-S. Wang, and Z.-B. Su, *Phys. Rev. B*. **2008**, 77, 235421
18 K. H. Michel, and B. Verberck, *Phys. Rev. B*. **2008**, 78, 085424
19 H. Wang, Y. F. Wang, X. W. Cao, M. Feng, and G. X. Lan, *J. Raman Spectrosc*. **2009**, 40, 1791
20 L. J. Karssemeijer,and A. Fasolino, A. *Surf. Sci*. **2011**, 605, 1611
21 K. H. Michel, and B. Verberck, *Phys. Rev. B*. **2012**, 85, 094303
22 F. Herziger, P. May, and J. Maultzsch, J. *Phys. Rev. B*. **2012**, 85, 235447
23 K. Sato, J. S. Park, R. Saito, C. Cong, T. Yu, C. H. Lui, T. F. Heinz, G. Dresselhaus, and M. S. Dresselhaus, *Phys. Rev. B*. **2011**, 84, 035419
24 C. H. Lui, L. M. Malard, S. Kim, G. Lantz, F. E. Laverge, R. Saito, and T. F. Heinz, *Nano Lett*. **2012**, 12, 5539
25 J. Shang, C. Cong, J. Zhang, Q. Xiong, G. G. Gurzadyana and T. Yu. *J. Raman Spectrosc*. **2012**, 44, 70
26 W.-H. Park, M. Jung, J.-S. Moon, S. Noh, T. H. Kim, M. Joo, K. Park. *Appl. Phys. Lett*. **2013**, 103, 071903
27 Y. Fang, Y. Huang, *Appl. Phys. Lett*. **2013**, 102, 153108
28 J. Chen, W. Yang, K. Dick, K. Deppert, H. Q. Xu, L. Samuelson, and H. Xu, *Appl. Phys.Lett*. **2008**, 92, 093110
29 G. Braun, S. J. Lee, M. Dante, T-Q. Nguyen, M. Moskovitz, N. Reich, *J. Am. Chem. Soc*. **2007**, 129, 6378
30 K. Kim, J. K. Yoon, *J. Phys. Chem. B*. **2005**, 109, 20731
31 J. Zheng, Y. Zhou, X. Li, Y. Ji, Y, Y. Lu, R. Gu, *Langmuir*. **2003**, 19, 632
32 W.- H. Park, S.-H. Ahn, Z. H. Kim, *ChemPhysChem*. **2008**, 9, 2491
33 K. S. Kim, Y. Zhao, H. Jang, S. Y. Lee, J. M. Kim, K. S. Kim, J.-H. Ahn, P. Kim, J.-Y. Choi, B. H. Hong, *Nature*. **2009**, 457, 706
34 C. H. Lui, T. F. Heinz, *Phys. Rev. B*. **2013**, 87, 121404(R)
35 W.-H. Park, Z. H. Kim, *Nano Lett*. **2010**, 10, 4040